Proceedings of the 2017 Winter Simulation Conference
W. K. V. Chan, A. D'Ambrogio, G. Zacharewicz, N. Mustafee, G. Wainer, and E. Page, eds.

DISH SIMULATOR: CAPTURING DYNAMICS OF CELLULAR SIGNALING WITH HETEROGENEOUS KNOWLEDGE

Khaled Sayed

Electrical and Computer Engineering
University of Pittsburgh
3700 O'Hara Street
Pittsburgh PA 15261, USA

Yu-Hsin Kuo

Language Technologies Institute
Carnegie Mellon University
5000 Forbes Ave
Pittsburgh PA 15213, USA

Anuva Kulkarni

Electrical and Computer Engineering
Carnegie Mellon University
5000 Forbes Ave
Pittsburgh PA 15213, USA

Natasa Miskov-Zivanov

Electrical and Computer Engineering
University of Pittsburgh
3700 O'Hara Street
Pittsburgh PA 15261, USA

ABSTRACT

In this paper, we present DiSH, a simulator for large discrete models of biological signal transduction pathways, capable of simulating networks with multi-valued elements in both deterministic and stochastic manner. The simulator incorporates the timing of molecular reactions, which are often not synchronized and occur in random order, and it also takes into account the difference between slow and fast reactions. DiSH also allows for changes in conditions during simulations, combined deterministic and stochastic changes, and it uses the concept of delays in models, similar to delays in digital circuits. DiSH is publicly available and has been used to study intra- and inter-cellular models of several diseases. It is also being used as part of a larger architecture including natural language processing tools that read biological literature, automated model assembly tools, and formal model analysis tools.

1 INTRODUCTION

Biological signaling pathways consist of molecules that interact with each other to convey signals inside and outside the cell (Gomperts, Kramer, and Tatham 2009). To study the *behavior* of pathway components or an overall system changes in time, as a response to external signals or internal perturbations, executable models are built and simulated. Executable models implement pathway components as variables, and interactions as variable update functions. Models may also contain quantitative information about reaction rates and component concentrations. The simulations start with specified initial conditions that represent particular pathway or cell state, and continue by executing update functions of model elements until desired state is observed, or until the model reaches steady state.

Executable models of cellular signaling pathways can be either continuous or discrete. Continuous models contain quantitative information such as concentrations of reactants and products and reaction rates. An example of a continuous model is an Ordinary Differential Equations (ODE)-based model. The continuous

models require the parameters of the system being modeled to be known. However, the information about mechanisms of component interactions and their parameters is often not available, or the modeler might prefer not to use all of the information available due to computational limitations. In these cases, discrete modeling approach is often more suitable.

It has been shown that Boolean models, a special case of discrete models, are capable of capturing characteristic dynamic behavior such as multi-stability, excitation and adaptation behavior (Albert and Robeva 2015). Positive and negative feedback and feed-forward loops can also be implemented in these models (Miskov-Zivanov et al. 2013). Incomplete information can be dealt with by using indirect causal evidence, which is not possible in ODE models or reaction rule-based models (Faeder, Blinov, and Hlavacek 2009). In discrete models, each element is assigned a set of discrete values representing activity of the modeled system component, as well as an update rule, which is a function of element's regulators.

Dynamic model analysis approaches have been developed previously (Danos et al. 2008, Faeder, Blinov, and Hlavacek 2009, Gillespie 1977, Kochańczyk et al. 2017). Several of these tools are used particularly for simulating Boolean models and some packages allow multi-valued modeling as well (Di Cara et al. 2007, Gonzalez et al. 2006, Hinkelmann et al. 2011). The *timing* of component changes is an important consideration in biological simulations. Different biological processes and reactions taking place inside a cell and in the cell environment are not synchronized and can even happen at different time scales. Furthermore, some components and pathways in modeled systems are well studied such that their mechanistic details are available, while other parts of the system are less known or not well understood. Finally, the speed of simulations remains critical, especially when simulation is a part of a larger framework. One such recent example includes automated information extraction, assembly of many model variants, model selection and analysis, with a feedback to guide further information extraction when needed, for the purpose of system understanding, explanation and prediction (Miskov-Zivanov 2015). Discrete modeling approach has been shown to be advantageous in all these situations (Miskov-Zivanov, Wei, and Loh 2014).

In this paper, we present our simulator, DiSH (Discrete, Stochastic, Heterogeneous model simulation), a stochastic simulator for discrete models with heterogeneous elements and interactions. DiSH implements multiple simulation schemes, and allows for fast simulation of discrete models. Compared to other existing simulators (Albert et al. 2008, Bock et al. 2014, Danos et al. 2008, Faeder, Blinov, and Hlavacek 2009, Gonzalez et al. 2006, Helikar and Rogers 2009, Müssel, Hopfensitz, and Kestler 2010, Yu et al. 2012, Zheng et al. 2010), our contribution with DiSH is two-fold: **(1)** We developed a representation that allows for multi-valued hierarchical models to be translated into logic circuit-like models and used by our simulator; **(2)** We incorporated rates of biological processes by associating probabilities with element update rules.

2 BACKGROUND

The construction of a model begins with identifying key signaling pathways of the modeled system, and the components on these pathways. Formally, let **E** be a set of all *model elements* (i.e., graph nodes), $\mathbf{e}_i \in \mathbf{E}$, i=1,..,*N*, where $N=|\mathbf{E}|$, that represent the system components. For each model element, we determine its *influence set*, which includes the element's positive and negative regulators, also called activators and inhibitors, respectively. The influence sets can be illustrated as *interaction maps* (graphs), where nodes represent model elements and edges represent regulatory interactions between elements. In Figure 1(a), we show an example interaction map of the CD4+ T-cell model from (Miskov-Zivanov et al. 2013). We also determine the number of *discrete levels*, v_i, that each element, $\mathbf{e}_i$, can take. These values represent the number of *discrete states* that a system component is observed to have.

Next, we assign to each element $\mathbf{e}_i$ a set of Boolean variables $E_{i,m}$, and their corresponding update functions $f_{E_{i,m}}$, where m=0,..,M_i and $M_i = (\log_2 v_i)$-1. The variables and their update rules comprise *executable*

model that is used by our simulator. Elements often have only two states: high activity or concentration (1 or True or ON value of Boolean variable) and low activity or concentration (0 or False or OFF value of Boolean variable). In this case, elements are assigned a single Boolean variable. However, model elements are not restricted to Boolean states, and can have multiple states that are then encoded with multiple Boolean variables. This allows modelers to encode multiple levels relevant to element's downstream activity, rather than encoding only two levels, while still utilizing logical model simulators and their benefits (Miskov-Zivanov et al. 2011). For example, element Phosphoinositide 3-kinase (PI3K) from the T-cell model in Figure 1(a), from (Miskov-Zivanov et al. 2013) has three states, representing the three observed levels of interest of PI3K in T cells, namely LOW, MEDIUM and HIGH. Therefore, PI3K element from the influence map in Figure 1(a) is represented in the executable model using two variables $PI3K_1$ and $PI3K_0$. Note that the combinations of variable $PI3K_1$ and $PI3K_0$ values are 00, 01, 10 and 11, where only three of these combinations are used to represent the three states of the PI3K node. For example, $(\mathrm{PI3K}_1, \mathrm{PI3K}_0) = 00, 01, or\ 10$ when PI3K is LOW, MEDIUM, or HIGH respectively.

This will be the case whenever $\log_2$ of the number of modeled levels is not an integer. In such cases, we will round $\log_2$ of the number of levels to the next integer. The additional variable value combinations obtained due to rounding ($(PI3K_1,PI3K_0) = 11$ in the case of PI3K) are either prohibited by the construction of the model, or made redundant by assigning them to one of the existing states. For example, since PI3K has only three states (LOW, MEDIUM and HIGH), the combination $(PI3K_1,PI3K_0) = 11$ will never occur in the model in (Miskov-Zivanov et al. 2013).

Furthermore, the number of discrete values in a regulated element and the number of discrete values in its regulators do not have to be same. For example, in Figure 1(a), the binary-valued element Mammalian Target of Rapamycin Complex 1 (mTORC1) can be active or inactive based on the values of its regulators, PI3K and Ribosomal protein S6 kinase beta-1 (S6K1). Note that S6K1 is also a binary-valued element, and therefore it requires a single Boolean variable, while PI3K is encoded with two Boolean variables, $PI3K_1$ and $PI3K_0$, each one having its own update rule. More formally, the value, $\mathbf{E}_i$, of a multi-valued element $\mathbf{e}_i$ is computed as:

$$\mathbf{E}_i = E_{i,0} \cdot 2^0 + \cdots + E_{i,\mathrm{M}_i} \cdot 2^{\mathrm{M}_i}. \tag{1}$$

The next value of variable $E_{i,m}$, at time step t+1, $E_{i,m}^{t+1}$, can be computed as a function of regulators of element $\mathbf{e}_i$ at time t, that is, as a function of Boolean variables corresponding to the regulators of $\mathbf{e}_i$:

$$\mathbf{E}_{i,m}^{t+1} = f_{E_{i,m}}\left(E_{1,0}^t,..,E_{1,\mathrm{M}_1}^t,E_{2,0}^t,..,E_{2,\mathrm{M}_2}^t,..,E_{N,0}^t,..,E_{N,\mathrm{M}_N}^t\right). \tag{2}$$

Next, we also define here a function $f_{\mathbf{e_i}}^t$, that determines the value of element $\mathbf{e}_i$ at time step t, from its component functions $f_{E_{i,m}}^t$:

$$\mathbf{E}_i^{t+1} = f_{\mathbf{e_i}}^t = f_{E_{i,0}}^t \cdot 2^0 + \cdots + f_{E_{i,\mathrm{M}_i}}^t \cdot 2^{\mathrm{M}_i} \tag{3}$$

In Figure 1(b), we show a toy example of interaction map that we will use throughout the paper to explain features of our simulator. The example includes three elements, that is, their corresponding Boolean variables and, for each variable, a logic update rule from the executable model. Multiple regulators can be combined in element update rule to compute the next state of element. The update rule is composed of variables corresponding to element's regulators, and of logic operators, AND, OR and NOT. A change in the state of regulators is reflected in the change of the regulated element, according to the logic combining regulators in the update rule – negatively (NOT), independently (OR), or with conditional dependence (AND). The creation of logic rules is described in (Miskov-Zivanov, Marculescu, and Faeder 2013). We have developed software which can derive logic update rules for all model variables according to influence set notation (determine when to use logic operators AND, OR, NOT). The details of the notation are beyond the scope

of this paper. Finally, given that logical models do not represent the time of biological events in the same manner as ODE models, methods exist to incorporate timing into these models (Miskov-Zivanov, Wei, and Loh 2014). Our simulation schemes described in the next section are designed to account for these delay modeling methods.

3 SIMULATION SCHEMES

In this section, we describe model execution schemes that our simulator supports (also shown in Figure 1(c)). Two main categories of simulation schemes are supported by DiSH: *Simultaneous* (SMLN), also sometimes referred to as synchronous, and *Sequential (*SQ*)*, also referred to as asynchronous scheme. As shown in Figure 1(c), in the SQ scheme, elements can be updated using either *Ranked-order* (RKSQ) or *Random-order* (RSQ) scheme. In addition, the selection of an element to be updated next in the RSQ scheme can be done in two ways: *Round-based (*RB-RSQ*)* selection and *Step-based (*SB-RSQ*)* selection, as described in the subsequent sections. The probability of selecting a rule to be updated in the SB-RSQ scheme can be *Uniform* (USB-RSQ), that is, the same probability value is assigned to each logic rule, or *Non-Uniform* (NUSB-RSQ), where the assigned probability is different for each rule.

Formally, the following holds for all the simulation schemes that we use. Let £ be the set of all possible states of the system, then we can compute the size of £ as: $|£| = v_1 \cdot v_2 \cdot \ldots \cdot v_N$ where v_i is defined in Section 2. In general, the probability $p(\mathbf{S}^{t+1}=\mathbf{S}_k)$ that, at time step t+1, the state $\mathbf{S}$ of the overall model is equal $\mathbf{S}_k$, where k is an integer between 1 and |£|, can be computed as:

$$p(\boldsymbol{S}^{t+1} = \mathbf{S}_k) = \sum_{l=1}^{|£|} p(\boldsymbol{S}^{t+1} = \mathbf{S}_k | \boldsymbol{S}^t = \mathbf{S}_l) \cdot p(\boldsymbol{S}^t = \boldsymbol{S}_l) \tag{4}$$

Furthermore, the probability that element $\mathbf{e}_i$ will take value V_j where j=0,..,v_i-1in time step t+1 during simulation, $p(\mathbf{E}_i^{t+1} = V_j)$, is then given by the following equation:

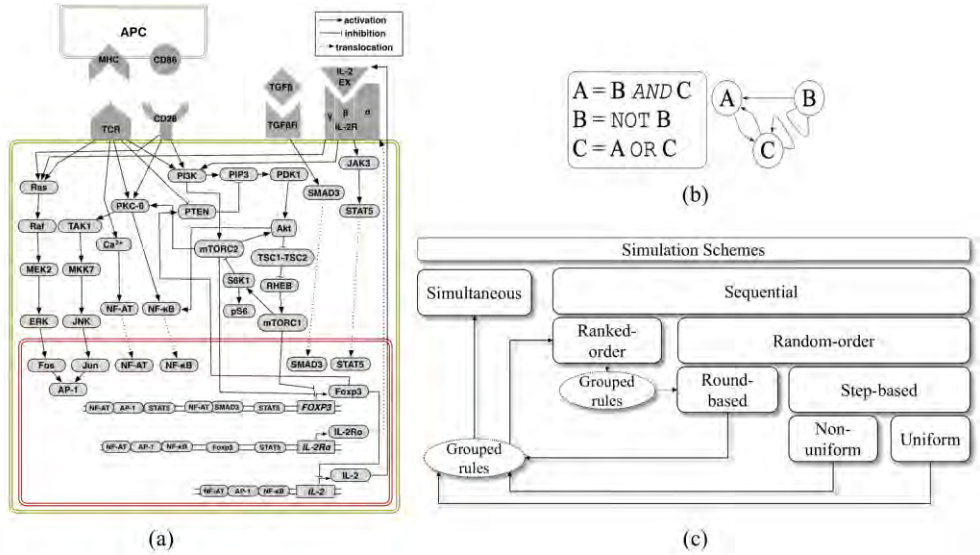

Figure 1: (a) An interaction map of the T-cell model from (Miskov-Zivanov et al. 2013). (b) A toy example: three nodes (A, B and C), and their update rules specified. (c) Simulation schemes.

$$p\left(\mathbf{E}_i^{t+1} = \mathrm{V}_j\right) = P_{\mathbf{e}_i} \cdot p\left(f_{\mathbf{e_i}}^t = \mathrm{V}_j\right) + (1 - P_{\mathbf{e}_i}) \cdot p\left(\mathbf{E}_i^t = \mathrm{V}_j\right) \quad (5)$$

where $P_{\mathbf{e}_i}$ represents the probability that element $\mathbf{e}_i$ is selected to be updated next, and $f_{\mathbf{e_i}}^t$ is the update function for element $\mathbf{e}_i$ at time step t during simulation. Then, $p\left(f_{\mathbf{e_i}}^t = \mathrm{V}_j\right)$ can be computed as:

$$p\left(f_{\mathbf{e_i}}^t = \mathrm{V}_j\right) = \sum_{l=1}^{|\mathfrak{L}|} p\left(f_{\mathbf{e_i}}^t = \mathrm{V}_j | \mathbf{S}^t = \mathbf{S}_l\right) \cdot p(\mathbf{S}^t = \mathbf{S}_l) \quad (6)$$

Therefore, one can then compute the probability of state $\mathbf{S}^{t+1}$ being equal to state $\mathbf{S}_k = (\mathrm{V}_{k,1}, \mathrm{V}_{k,2}, \ldots, \mathrm{V}_{k,N})$, where $\mathrm{V}_{k,i}$ is the value of element $\mathbf{e}_i$ in state $\mathbf{S}_k$, as:

$$p(\mathbf{S}^{t+1} = \mathbf{S}_k) = \prod_{i=1}^{N} p\left(\mathbf{E}_i^{t+1} = \mathrm{V}_{k,i}\right) \quad (7)$$

3.1 Simultaneous (SMLN) Scheme

In the SMLN scheme, all elements are updated simultaneously, that is, current state values of all variables are used to simultaneously compute next state values. SMLN scheme is therefore deterministic: for each state, there is only one possible next state. In SMLN, if an initial state of the system is given, one can determine the steady state or steady cycle that the system will reach. In other words, the probability $P_{\mathbf{e}_i}$ from equation (5) is equal 1 for all elements $\mathbf{e}_i$, and in each given time step t, the probabilities $p(\mathbf{S}^t = \mathbf{S}_l)$ will be equal 0 for all but one value l=L, for which it will be $p(\mathbf{S}^t = \mathbf{S}_\mathrm{L}) = 1$. A state transition graph (STG) resulting from the simulation of our toy example from Figure 1(c), using the SMLN scheme, is depicted in Figure 2(a). Given elements of the toy model, A, B, C, and their corresponding values, $\mathrm{V_A}$, $\mathrm{V_B}$, $\mathrm{V_C}$, if the simulation starts at time t=0 we denote this as state $\mathbf{S}^0 = (\mathrm{V_A}^0, \mathrm{V_B}^0, \mathrm{V_C}^0)$. The probability of the following states $\mathbf{S}^{t+1} = \mathbf{S}_k$ for time steps t=0,..,n where n is the number of simulation steps, will in each time step be equal 1 for one specific k=K$_t$, and will be 0 for all other $k \neq$ K$_t$. For example, in our toy system, as shown in Figure 2(a), if the simulation starts from any state except states 000 and 010, we will always reach state 101, and the model will then oscillate between states 011 and 101. In addition, if the simulation starts at state 000 or 010, it keeps oscillating between these two states and never moves to any other state.

3.2 Random-order Sequential (RSQ) Scheme

In the RSQ scheme, model variables are not updated simultaneously, instead they are updated sequentially and in random order. In other words, once element $\mathbf{e}_\mathrm{i}$ is updated in time step t by computing its new value according to its update function $f_{\mathbf{e_i}}$, this new value is used to determine model element values in the following time steps until the same element $\mathbf{e}_\mathrm{i}$ is selected for update again. This scheme allows for modelling cellular signaling and processes in a more realistic way than in the SMLN scheme, as it accounts for the randomness that exists in the timing of biological events. The STG of our toy example system, when simulated using the RSQ scheme, is shown in Figure 2(b). As can be seen from the STG, a state can have multiple next states, and thus, a given initial state can be followed by multiple different paths through STG and result in different steady-states. This means that the probability $P_{\mathbf{e_i}}$ from equation (5) does not have to be equal 1 for a given element $\mathbf{e}_\mathrm{i,}$ in a given time step t, as it was the case in the SMLN scheme. Instead, this probability will depend on the method used for selecting elements for update, as described in the following subsections. Furthermore, in each given time step t, the probabilities $p(\mathbf{S}^\mathrm{t} = \mathbf{S}_l)$ can vary between 0 and 1 for different values of l.

3.2.1 Round-Based Random-order Sequential (RB-RSQ) Scheme

The RB-RSQ simulation scheme has been previously described in (Albert et al. 2008, Li, Assmann, and Albert 2006) and used in (Miskov-Zivanov et al. 2013). It is important to distinguish here between simulation *step* and simulation *round*. While the simulation step accounts for updating value of a single element, and can also correspond to time step in our earlier discussion, the simulation round represents a cycle within which **all** elements are updated **exactly once** according to their update functions. Formally, if a model has N elements, $\mathbf{e}_i$, i=1,..,N, and their update functions are $f_{\mathbf{e}_i}$, then each round consists of N steps, ROUND = (STEP$_1$,...,STEP$_N$), and in each round a new random order is determined, in which the values of these function are computed. Thus, in a given round T, the element update order is a random permutation P_r of the vector (STEP$_1$,...,STEP$_N$): update_order$_T$ (E) = (STEP$_{T1}$,...,STEP$_{TN}$) = P_r(STEP$_1$,...,STEP$_N$) such that the step at which element $\mathbf{e}_i$ is updated is STEP$_{Ti}$. Given that every element gets updated exactly once within a round, the probability $P_{\mathbf{e}_i}$ that an element $\mathbf{e}_i$ is selected for update in a given time step t depends on the STEP$_{Ti}$ within round when this update occurs: $P_{\mathbf{e}_i} = 1/\left(N - \left(STEP_{T_i} - 1\right)\right)$. The two simulation rounds when the RB-RSQ method is applied to our toy example starting at state 100 are shown in Figure 2(c).

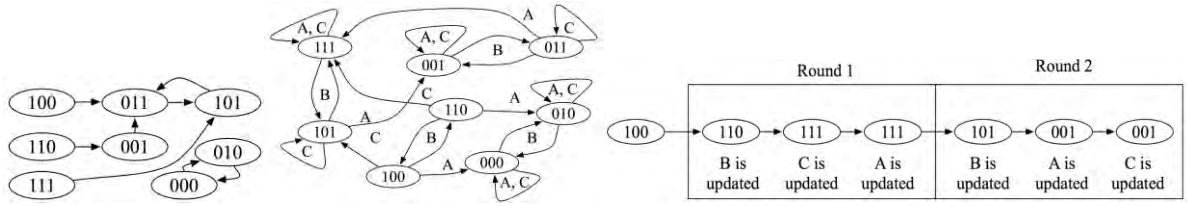

Figure 2. STG for the toy example in Figure 1, for (a) the SMLN scheme and (b) the RSQ scheme. Labels on graph edges indicate which elements are selected for update. (c) RB-RSQ scheme.

3.2.2 Step-Based Random-order Sequential (SB-RSQ) Scheme

In the SB-RSQ simulation scheme, one model element is chosen for update in each time step. There are no round-based restrictions for element selection, and therefore, the same element can be updated in consecutive steps. In addition, elements can be chosen for update all at the same rate or at different rates. Thus, we define the following two sub-schemes.

*Uniform (*USB-RSQ*):* In this simulation approach, all elements have the same update rate, and for a model with N elements, in each step the probability for an element $\mathbf{e}_i$ to get selected for update is: $P_{\mathbf{e}_i} = 1/N$

This approach is used when the time scales of changes in system elements are not well known, and thus the default approach is to assume that the rates at which elements are updated are equal.

*Non-uniform (*NUSB-RandSeq*):* In this simulation approach, each model element **e**i has an assigned update rate , $r_{\mathbf{e}_i}$. We assign update rates to elements based on prior knowledge, such that the system evolves over

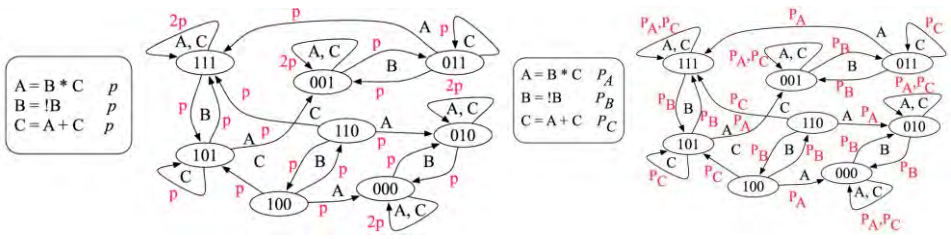

Figure 3. Logic rules and STG in the (a) USB-RSQ and (b) NUSB-RSQ scheme.

time following the rate of change observed in experiments. For example, since gene transcription and translation occur at a different time scale compared to protein modifications, we assign higher rates to protein interactions and lower rates to gene activation and protein synthesis. In this simulation approach, the probability of element being selected next for update is a function of these update rates: $P_{\mathbf{e}_i} = \frac{r_{\mathbf{e}_i}}{\sum_{i=1}^{N} r_{\mathbf{e}_i}}$ where the probability of selecting an element **e**i to update its rule is proportional to the sum of all update rates in the model. We illustrate both types of SB scheme, USB and NUSB, in Figure 3(a) and (b).

3.3 Ranked-order Sequential (RKSQ) Scheme

Element update rules can also be assigned *rank numbers*. This feature is adopted from the BooleanNet tool developed by (Albert et al. 2008). Those rules that have same rank are executed using RB-RSQ scheme. Similarly, groups with different rank are executed according to their rank: all rules in the group with rank 1 are executed first, then all the rules with rank 2 are executed, and so on. As shown in Figure 4(a)(left), B and C should be updated first in random order before we update A which has rank 2.

3.4 Additional Functionalities

3.4.1 Grouped rules

Often, we are interested in grouping some variables together such that they are updated either simultaneously, or in the order in which they are listed in the model file. Examples of such situations are (i) all Boolean variables $E_{i,m}$ representing the *same model element* $\mathbf{e}_i$ are grouped and updated simultaneously; (ii) if there are *different model elements* that need to be updated at the same time, all their corresponding variables will be grouped and updated simultaneously; (iii) if it is required for a group of different model elements or for a group of model variables corresponding to the same element to be updated in a specific order, but in random order with the other elements or variables in the model, they are grouped and executed sequentially, in the order in which their update rules are listed in the model file. The update rules of all variables that need to be updated together are specified within curled braces '{}' in the model file. In the SMLN scheme, this does not change the execution of rules, since the grouped rules are executed at the same time with the other rules. However, in the SQ scheme, the grouped rules are executed together when the group is selected to be updated at a specific time step. Figure 4(b) shows an example where nodes A and C are grouped. The difference in resulting simulated model behavior is illustrated with two state diagrams when the first (initial) state is the same, as shown in Figure 4(c).

3.4.2 Toggle implementation

It is possible to toggle the value of a variable (i.e., switch from 1 to 0 and from 0 to 1) at a specific round or step by specifying this in the model file next to the variable initialization. This is often a useful feature

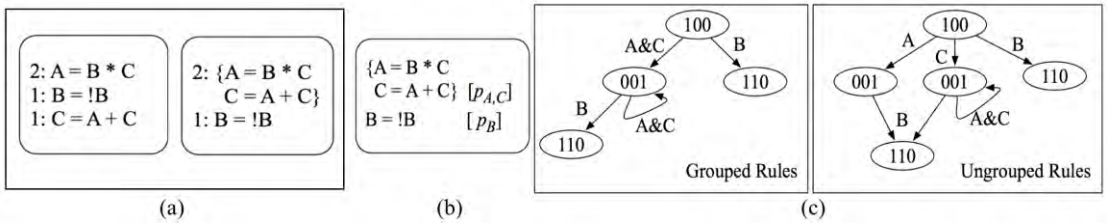

Figure 4. (a) (left) Ranked rules and (right) Ranked rules with grouping. (b) The syntax for grouped rules. (c) Two small examples of the state diagrams when grouped rules are used.

of simulations that allows us to closely mimic wet-lab experiments. For example, toggling the value of the T-cell receptor (TCR) signal in the T-cell model allows for studying the impact of the duration of a high signal on the system's behavior. This functionality should be used with the RSQ simulation schemes.

4 SIMULATION RESULTS

In the following discussion we will refer to ***run*** as a single simulation run from the starting point, when we assign initial values to all variables, through a pre-determined number of rounds or number of steps (depending on the simulations scheme used). A *trajectory* of values is obtained for each element in the run, and the trajectories may vary across consecutive runs. The values for variables in each round or step are averaged over all the runs and this *average trajectory* can be plotted for analysis.

4.1 Case study – T cell differentiation model

In this section, we illustrate different simulation schemes that are implemented within our DiSH simulator using the T-cell differentiation model from (Miskov-Zivanov et al. 2013). The stimulation of naïve peripheral T cells occurs via antigen presentation to T cell receptor (TCR), and with co-stimulation at CD28 receptor. These two stimulatory signals lead to activation of several pathways, of feedback and feedforward loops between pathway elements, and eventually result in differentiation of naïve T cells into helper (Th) or regulatory (Treg) phenotype. It has been shown that the ratio between Th and Treg cells in the T cell population strongly depends on antigen dose where high antigen dose results in mostly Th cells, while low antigen dose leads to mixed population of Th and Treg cells. Therefore, TCR is modeled in (Miskov-Zivanov et al. 2013) as having three different values, no stimulation (value 0, or LOW), stimulation with low antigen dose (value 1, or MEDIUM), and stimulation with high antigen dose (value 2, or HIGH). According to the description in Section 2, element TCR is implemented in the executable model using two Boolean variables, TCR_{HIGH} and TCR_{LOW}. Furthermore, the duration of the presence of the high signal (high antigen dose, TCR_{HIGH}=1) has been shown to be critical in phenotype decision (Miskov-Zivanov et al. 2013).

Here, we simulate two main scenarios; Scenario I, which includes 5 sub-scenarios, and Scenario II, which includes 3 sub-scenarios, all of them listed in Figure 5(g). The five sub-scenarios under Scenario I consider low and high levels of antigen dose (TCR_{HIGH}=0 and TCR_{LOW}=1, TCR_{HIGH}=1 and TCR_{LOW}=0, respectively), as well as different initial values of proteins TGF-β and AKT, also responsible for regulating the T-cell differentiation. It has been shown that the addition of TGF-β bypasses the suppression of Foxp3 under the condition of high antigen dose (Miskov-Zivanov et al. 2013), while the removal of AKT induces the expression of Foxp3 and enhances the differentiation into Treg cells (Sauer et al. 2008). On the other hand, the three sub-scenarios of Scenario II consider the antigen dose removal at certain time steps to reflect the impact of the time at which the high antigen dose is removed during the wet-lab experiments on the differentiation outcomes of naïve T cells. The removal of the high antigen dose is simulated by toggling the value of the TCR_{HIGH} variable from 1 to 0 at specific simulation steps, which changes the value of the TCR variable from HIGH to LOW.

4.2 Comparison between different simulations schemes

In the subsequent sections, we show the simulation results obtained by running the simulator using the simulation schemes that were described in Section 3, for Foxp3 only due to the limited space. However, we discuss the response of Foxp3 in terms of other key elements such as IL-2, mTORC1, CD25, and STAT5, for the scenarios shown in Figure 5(g). These 5 model elements were selected to describe the outcomes of the naïve T cells differentiation process into Th and Treg cells, where Th cells are characterized by the high

expression of IL-2 and low expression of Foxp3, while the Treg cells are characterized by the high expression of Foxp3 and low expression of IL-2 (Miskov-Zivanov et al. 2013). In addition, mTORC1 is a key player in the inhibition of Foxp3 at high antigen dose, while the early activation of Foxp3 by CD25/STAT5 pathway is an essential requirement for the differentiation of the naïve T cells into Treg cells at low antigen dose (Miskov-Zivanov et al. 2013).

The SMLN scheme is deterministic as each state has only one possible next state. All variable values at time $t+1$ are computed using the values of their regulators at time t. The SMLN scheme computes steady-states that the system can reach, but it cannot account for the randomness of occurrence of events that is common for biological systems. In Figure 5(a), we show the simulation results for Scenarios I using the SMLN scheme. The T cell model is simulated 1000 times (i.e., 1000 runs), each run consisting of 50 steps, assuming random initial values for all elements, except for TCR, TGF-β and AKT which were selected to satisfy the requirements of each sub-scenario in Figure 5(g). It can be seen that the steady-state value of Foxp3 in sub-scenario I1 (high antigen dose) is lower than the steady-state value in sub-scenario I2 (low antigen dose), which was expected, according to (Miskov-Zivanov et al. 2013). However, the steady-state value of Foxp3 is not very low in sub-scenario I1 because the expression level of STAT5 and CD25 is high (activators of Foxp3), even with high expression level of mTORC1 (inhibitor of Foxp3). Also, we can see some oscillations in the transient response of Foxp3 in Figure 5(a), which arise from the random initializations of the model elements enabling each simulation run to start from a different state, i.e., a different point in the state space. Additionally, these plots show that the SMLN scheme is useful for quickly identifying different steady-states that the system can reach. However, the SMLN scheme may not provide accurate trajectories for studying the transient response of the system, as it does not account for the stochasticity in the biological systems.

A more detailed analysis can be performed using RSQ scheme, which computes transient behavior of elements, and provides a better resolution of small changes occurring on element trajectories. As described in Section 3.2, the RSQ scheme has two sub-types, round-based (RB-RSQ) and step-based (SB-RSQ) schemes. Here, we show simulation results using the RB-RSQ scheme for all sub-scenarios of Scenario I, where the value of each element is updated once per round according to the element's update rule. The results of our DiSH simulator are in agreement with those presented in(Miskov-Zivanov et al. 2013), that were obtained using the simulator described (Albert et al. 2008). As shown in Figure 5(b), the steady-state value of Foxp3 is low (high) in scenario I1 (I2) which represents the high (low) antigen dose. In addition, Foxp3 exhibits a transient increase at high antigen dose (Scenario I1), due to the activation of CD25 and STAT5. This increase of the Foxp3 activation is quickly turned off because of the activation of mTORC1, which is a Foxp3 inhibitor. We can also see that initializing TGF-β at high level, with low antigen dose stimulation (Scenario I4) can provide a rapid increase in the Foxp3 expression, which inhibits any transient response of IL-2. The other sub-type of the RSQ simulation scheme is the SB-RSQ scheme which has also two sub-types, the uniform (USB) and non-uniform (NUSB) probability simulation schemes. The simulation results for Scenario I with the USB-RSQ scheme are shown in Figure 5(c). The simulation results in Figure 5(c) are similar to the ones in Figure 5(b), where the RB-RSQ scheme was used, except that the transient responses shown in Figure 5(c) are delayed. This is happening due to the nature of the updating scheme. So, while each element gets updated once per round in the RB-RSQ scheme, only one element is updated in a step in the SB-RSQ scheme. Due to such updating schemes, the RB simulations will show faster rates of change than the SB ones. In the RB simulation, the number of time steps in each round is equal to the number of variables. In the T cell model, there are 61 variables, and in each of the 50 rounds, each variable is updated 50 times. On the other hand, in the step-based simulation, it may take more than 50 steps to update all elements because some elements may be updated several times within those 50 steps,

while some other elements will not get updated. Figure 5(c) also emphasizes an interesting biological finding which was confirmed by the experimental results in (Miskov-Zivanov et al. 2013), suggesting that initializing TGF-β at high even with high antigen dose stimulation (Scenarios I3 and I4) will produce more Treg cells.

As described previously, in the NUSB-RSQ scheme, in each time step one variable is chosen for update according to the assigned update probabilities. When studying the T cell model using this scheme, we divide all the variables of the T-cell model into two blocks. Block A contains CD25, Foxp3 and IL2 variables, and has lower probability value, which is 0.1, and Block B, which contains the rest of the variables, is assigned probability 0.9. The blocks have been constructed using prior knowledge about the biological system – it is known that protein-protein interactions (Block B) occur at a faster speed than transcription reactions in Block A (such as transcription of the *FOXP3* gene in the nucleus). Figure 5(d) shows that we get fast transient responses for Foxp3 because of the fast transient response of the elements in Block B (i.e. STAT5 and mTORC1), which regulate Foxp3. However, the overall biological behavior of the system is almost the same as in the USB-RSQ scheme, with faster response since Block B elements are updated more often.

In the RKSQ simulation scheme, we can order the rules based on a priori knowledge about the sequence of the biological events. Here, we assign rank 1 for the rules that represent the cell membrane elements (e.g., TCR) and rank 2 for the elements that are regulated by the cell membrane elements, and we continue with the same procedure until we reach the last elements in the signaling pathway (e.g., gene transcriptions usually have the last rank). Figure 5(e) shows the simulation results for the sub-scenarios of Scenario I using the RKSQ scheme. The results for RKSQ are almost the same as the results shown in Figure 5(b), which were obtained using the RB-RSQ scheme, suggesting that the RKSQ scheme can be used if the information about the order of the biological events are known. Also, this shows that the RSQ scheme is able to capture the biological events even if the prior knowledge about the signaling events is not available.

Finally, we ran the simulator using USB-RSQ scheme for the three sub-scenarios II1, II2, and II3, when the TCR signal is turned off at simulation steps 100, 300, and 500, respectively. The simulation results in Figure 5(f) show that the time at which the TCR signal is turned off is critical for the T cell differentiation as confirmed by(Miskov-Zivanov et al. 2013). It can be seen that turning off the TCR signal at very early simulation step (e.g., Scenario II1) will lead to undifferentiated cells that are characterized by the low expression of both Foxp3 and IL-2. On the other hand, turning off the TCR signal at an intermediate step (e.g., Scenario II2) will cause the naïve T cells to be differentiated into Treg cells that are characterized by high

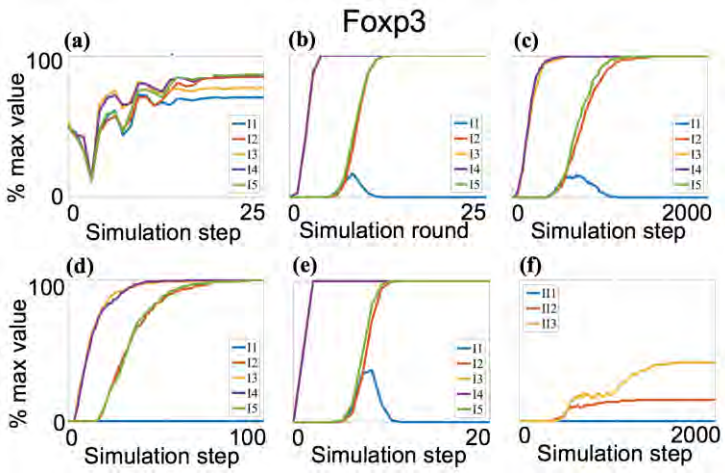

(g)

Scenario name	Description	Specific Conditions
I1	High Antigen dose	TCR_{HIGH} = True
I2	Low Antigen Dose	TCR_{LOW} = True
I3	High antigen dose and TGF-β is high	TCR_{HIGH}= True, TGF_{BETA} = True
I4	Low antigen dose and TGF-β is high	TCR_{LOW} = True, TGF_{BETA} = True
I5	High Antigen Dose and AKT is off	TCR_{HIGH} = True, AKT_{OFF} = True
II1	High antigen dose, toggle TCR_{HIGH}	Toggle at Step 100
II2	High antigen dose, toggle TCR_{HIGH}	Toggle at Step 300
II3	High antigen dose, toggle TCR_{HIGH}	Toggle at Step 500

Figure 5: Trajectories for Foxp3 using different simulation schemes:a) SMLN, b) RB-RSQ, c) USB-RSQ, d) NUSB-RSQ, e) RKSQ, f) Toggling feature with USB-RSQ, and g) A list of simulation scenarios.

expression of Foxp3. Additionally, turning off the TCR signal at later steps (e.g., Scenario II3) will produce more Th cells which are characterized by low expression of Foxp3. This behavior can be explained by looking at the trajectories of mTORC1 and CD25/STAT5 where the inhibition signal for Foxp3 through mTORC1 lasts longer when we remove the antigen dose at later simulation steps.

5 CONCLUSIONS

This paper describes the features of our biological system simulator, DiSH. While similar tools have been developed in the past, the contributions of DiSH include simulations of multi-valued model elements, grouping element update functions in several different ways, and the use of delays to simulate biological networks in a more realistic manner. DiSH is applicable to discrete (including logical) models of complex biological networks. The advantage of discrete models is that they do not necessarily require information about reaction rates and concentrations, which is often not available or impractical to use. Furthermore, the SMLN and RSQ simulation schemes in DiSH enable analysis of both dynamic system behavior and its attractors. Deterministic discrete model simulations that assume simultaneous element update enable quick attractor analysis. However, when we have prior knowledge about faster and slower events, simultaneous simulations are not a good choice. In the discrete modeling approach, we can incorporate a priori knowledge about observed difference in event rates using delays and probabilistic simulation. Therefore, our simulator allows scientists to look at biological systems from various perspectives, and learn more about the system by conducting multiple simulations under different conditions.

ACKNOWLEDGMENTS

This work is supported in part by DARPA award W911NF-14-1-0422.

REFERENCES

Albert, I., J. Thakar, S. Li, R. Zhang, and R. Albert. 2008. "Boolean Network Simulations for Life Scientists." *Source Code for Biology and Medicine* 3(1):16.

Albert, R., and R. Robeva. 2015. "Signaling Networks: Asynchronous Boolean Models." In *Algebraic and Discrete Mathematical Methods for Modern Biology*, edited by R. Robeva, Chapter 4, 65-91. Academic Press.

Bock, M., T. Scharp, C. Talnikar, and E. Klipp. 2014. "BooleSim: An Interactive Boolean Network Simulator." *Bioinformatics* 30(1):131-132.

Danos, V., J. Feret, W. Fontana, R. Harmer, and J. Krivine. 2008. "Rule-Based Modelling, Symmetries, Refinements." In *Formal Methods in Systems Biology*, 5054 (1):103-122. Springer.

Di C., Alessandro, A. Garg, G. De Micheli, I. Xenarios, and L. Mendoza. 2007. "Dynamic Simulation of Regulatory Networks using SQUAD." *BMC Bioinformatics* 8 (1):462.

Faeder, J. R., M. L. Blinov, and W. S. Hlavacek. 2009. "Rule-Based Modeling of Biochemical Systems with BioNetGen." *Systems Biology*:113-167.

Gillespie, D. T. 1977. "Exact Stochastic Simulation of Coupled Chemical Reactions." *J. Phys. Chem* 81 (25):2340-2361.

Gomperts, B. D., I. M. Kramer, and P. E. Tatham. 2009. *Signal Transduction*: Academic Press.

Gonzalez, A. G., A. Naldi, L. Sanchez, D. Thieffry, and C. Chaouiya. 2006. "GINsim: A Software Suite for the Qualitative Modelling, Simulation and Analysis of Regulatory Networks." *Biosystems* 84 (2):91-100.

Helikar, T., and J. A. Rogers. 2009. "ChemChains: A Platform for Simulation and Analysis of Biochemical Networks Aimed to Laboratory Scientists." *BMC Systems Biology* 3 (1):58.

Hinkelmann, F., M. Brandon, B. Guang, R. McNeill, G. Blekherman, A. Veliz-Cuba, and R. Laubenbacher. 2011. "ADAM: Analysis of Discrete Models of Biological Systems using Computer Algebra." *BMC Bioinformatics* 12 (1):295.

Kochańczyk, M., P. Kocieniewski, E. Kozłowska, J. Jaruszewicz-Błońska, B. Sparta, M. Pargett, J. G. Albeck, W. S. Hlavacek, and T. Lipniacki. 2017. "Relaxation Oscillations and Hierarchy of Feedbacks in MAPK Signaling." *Scientific Reports* 7:38244.

Li, S., S. M. Assmann, and R. Albert. 2006. "Predicting Essential Components of Signal Transduction Networks: A Dynamic Model of Guard Cell Abscisic Acid Signaling." *PLoS Biol* 4 (10):e312.

Miskov-Zivanov, N.. 2015. "Automation of Biological Model Learning, Design and Analysis." In *Proceedings of the 25th edition on Great Lakes Symposium on VLSI*, 327-329. ACM.

Miskov-Zivanov, N., A. Bresticker, D. Krishnaswamy, S. Venkatakrishnan, P. Kashinkunti, D. Marculescu, and J. R. Faeder. 2011. "Regulatory Network Analysis acceleration with Reconfigurable Hardware." In *Engineering in Medicine and Biology Society, EMBC, 2011 Annual International Conference of the IEEE*, 149-152. IEEE.

Miskov-Zivanov, N., D.Marculescu, and J. R. Faeder. 2013. "Dynamic Behavior of Cell Signaling Networks: Model Design and Analysis Automation." In *Proceedings of the 50th Annual Design Automation Conference*, 8. ACM.

Miskov-Zivanov, N., M. S. Turner, L. P. Kane, P. A Morel, and J. R. Faeder. 2013. "Duration of T cell Stimulation as a Critical Determinant of Cell Fate and Plasticity." *Science Signaling* 6 (300):ra97.

Miskov-Zivanov, N., P. Wei, and C. S. C. Loh. 2014. "THiMED: Time in Hierarchical Model Extraction and Design." In *International Conference on Computational Methods in Systems Biology*, 260-263. Springer, Cham.

Müssel, C., M. Hopfensitz, and H. A Kestler. 2010. "BoolNet—An R Package for Generation, Reconstruction and Analysis of Boolean Networks." *Bioinformatics* 26 (10):1378-1380.

Sauer, S., L. Bruno, A. Hertweck, D. Finlay, M. Leleu, M. Spivakov, Z. A. Knight, B. S. Cobb, D. Cantrell, and E. O'Connor. 2008. "T Cell Receptor Signaling Controls Foxp3 Expression via PI3K, Akt, and mTOR." In *Proceedings of the National Academy of Sciences* 105 (22):7797-7802.

Yu, S. J., T. Q. Tung, J. Park, J. Lim, and J. Yoo. 2012. "ezBioNet: A Modeling and Simulation System for Analyzing Biological Reaction Networks." *Journal of the Korean Physical Society* 61 (8):1267-1273.

Zheng, J., D. Zhang, P. F. Przytycki, R. Zielinski, J. Capala, and T. M. Przytycka. 2010. "SimBoolNet—A Cytoscape Plugin for Dynamic Simulation of Signaling Networks." *Bioinformatics* 26 (1):141-142.

AUTHOR BIOGRAPHIES

KHALED SAYED is a PhD student at the department of Electrical and Computer Engineering, university of Pittsburgh. His e-mail address is k.sayed@pitt.edu.

YU-HSIN KUO received his MS degree in Computer Science at Carnegie Mellon University in 2015. He is currently a software engineer at Facebook. His email address is yhsinkuo@gmail.com.

ANUVA KULKARNI is a PhD candidate at the Department of Electrical and Computer Engineering, Carnegie Mellon University. Her email address is anuvak@andrew.cmu.edu.

NATASA MISKOV-ZIVANOV is an Assistant Professor in Electrical and Computer Engineering at the University of Pittsburgh. Her email address is nmzivanov@pitt.edu.